Nickel hexacyanoferrate electrodes for high mono/divalent ion-selectivity in capacitive deionization

Singh, Kaustub; Qian, Zexin; Biesheuvel, P. M.; Zuilhof, Han; Porada, Slawomir; de Smet, Louis C.P.M.

DOI
10.1016/j.desal.2020.114346

Publication date
2020

Document Version
Final published version

Published in
Desalination

Desalination 481 (2020) 114346

Contents lists available at ScienceDirect

Desalination

journal homepage: www.elsevier.com/locate/desal

Nickel hexacyanoferrate electrodes for high mono/divalent ion-selectivity in capacitive deionization

Kaustub Singh[a,b,1], Zexin Qian[b,c,1], P.M. Biesheuvel[b], Han Zuilhof[a,d,e], Slawomir Porada[b,f], Louis C.P.M. de Smet[a,b,*]

[a] Laboratory of Organic Chemistry, Wageningen University, Stippeneng 4, 6708 WE Wageningen, The Netherlands
[b] Wetsus, European Centre of Excellence for Sustainable Water Technology, Oostergoweg 9, 8911 MA Leeuwarden, The Netherlands
[c] Department of Chemical Engineering, Delft University of Technology, Van der Maasweg 9, Delft 2629 HZ, The Netherlands
[d] School of Pharmaceutical Sciences and Technology, Tianjin University, Tianjin, China
[e] Department of Chemical and Materials Engineering, Faculty of Engineering, King Abdulaziz University, Jeddah, Saudi Arabia
[f] Soft Matter, Fluidics and Interfaces Group, Faculty of Science and Technology, University of Twente, Drienerlolaan 5, 7522 NB Enschede, The Netherlands

ARTICLE INFO

Keywords:
Ion-selective intercalation
Prussian blue analogues
Mono/divalent selectivity
Capacitive deionization

ABSTRACT

Selective ion removal has been a point of focus in capacitive deionization because of its industrial applications such as water purification, water softening, heavy metal separation and resource recovery. Conventionally, carbon is used as electrode material for selectivity. However, recent developments focus on intercalation materials such as Prussian Blue Analogues, due to their size-based preference towards cations. Selectivity of nickel hexacyanoferrate electrodes from a mixture of Na^+, Mg^{2+}, and Ca^{2+} ions was studied in this work. Here, a CDI cell with two identical NiHCF electrodes was operated in two desalination modes: (a) cyclic, in which ions are removed from and released into the same water reservoir and thus, the ion concentration remains the same after one cycle, and (b) continuous, in which ions are removed from one water reservoir and released back in a different reservoir. An average separation factor of ≈15 and 25, reflecting the selectivity of the electrodes, was obtained for Na^+ over Ca^{2+} and Mg^{2+} from an equimolar solution of Na^+, Ca^{2+} and Mg^{2+} in both, cyclic and continuous desalination. It was concluded that NiHCF, used in a symmetric CDI cell, is a promising material for highly selective removal of Na^+ from a multivalent ion mixture.

1. Introduction

Capacitive Deionization (CDI) is an electrochemical technique in which polarized electrodes remove ions from water [1,2]. Conventionally, these electrodes are fabricated out of porous carbon [3–7] with ions stored in micropores with sizes just above and below 1 nm. Recently, research into intercalation materials for aqueous ion batteries [8–10] has led to their application in CDI [11–15]. The ion storage in these materials proceeds via intercalation of ions into the interstitial lattice sites or in between the layers of the host electrode material. In some intercalation materials, such as Prussian Blue Analogues (PBAs) [16–18], the ion insertion is accompanied by the electrochemical reduction of a redox-active element in the lattice. These intercalation materials retain the attributes of porous carbon-based electrodes, such as a non-toxic nature, easy preparation, and fast charge transfer kinetics [16], while improving upon the charge adsorption capacity [19] and eliminating co-ion expulsion from the electrode [4]. The use of PBAs in CDI is of interest because of their open framework structure, customizable chemical composition, and size-based selectivity towards cations [20]. Selective removal of ions using CDI has already been explored with carbon electrodes [21–24]. Only recently, it has been studied with electrodes based on intercalation materials as well [25–27]. However, much of this focus has been on the separation between cations with the same valence, and very few studies are available on the selective removal of a cation from a mixture of ions with different valency. This contrasts with the research focus towards carbon electrodes, where selective removal of ions from a mixture has been extensively studied [28–31]. This work aims at filling this gap in literature.

The electrodes used for selective ion-removal here contain nickel hexacyanoferrate (NiHCF) particles as the active material. It is a PBA that has been successfully used for desalination [11,17] and was found

* Corresponding author at: Laboratory of Organic Chemistry, Wageningen University, Stippeneng 4, 6708 WE Wageningen, The Netherlands.
E-mail address: louis.desmet@wur.nl (L.C.P.M. de Smet).
[1] These authors contributed equally.

https://doi.org/10.1016/j.desal.2020.114346
Received 22 November 2019; Received in revised form 16 January 2020; Accepted 20 January 2020
Available online 06 February 2020

to a have size-based preference for cations in CDI [17] and other electro-chemical techniques [32–34]. In more detail, the trends observed for alkali metal ions suggest that the affinity of NiHCF particles towards ions decreases with an increase in their hydrated size in aqueous electrolytes. Studies [32,33,35] have shown that in a mixture of alkali metal ions, PB and its analogues demonstrate the strongest affinity towards Cs^+, and the affinity reduces for the alkali metals above Cs^+ in the group.

In this study, we demonstrate the performance of electrodes fabricated using NiHCF in CDI experiments to selectively remove monovalent (Na^+) over divalent (Ca^{2+}, Mg^{2+}) ions. The preferential removal of Na^+ from a mixture of Na^+, Ca^{2+}, and Mg^{2+} is crucial to maintain the quality of irrigation water as an increase in its Na^+ can result in adverse effects on the physical properties of soil [36] and plant growth [37,38]. This was achieved with a symmetric two-compartment CDI cell [39], constructed with two NiHCF electrodes of the same mass, and identical physical, chemical and electrochemical composition. These electrodes were separated by an anion-exchange membrane inside the cell. The use of identical electrode materials avoids the need for an anode with an equivalent charge storage capacity and allows for an uninterrupted selective ion removal in the adsorption and regeneration steps by reversing the electrode polarities. Part of the potential of the presented electrochemical setup lies in the cheap, non-toxic and facile fabrication of ion-selective NiHCF particles, and subsequently, of the electrodes, and in their easy application in a symmetric, two-compartment deionization cell. Fig. 1a illustrates the intercalation compartment of the symmetric desalination cell, illustrated elsewhere [40], during the operation. The other half of the cell undergoes a mirrored deintercalation operation simultaneously, evident from the outlet concentrations measured during the desalination cycles. The inset schematic indicates the size-based exclusion of cations by the NiHCF lattice.

2. Experimental section

2.1. NiHCF preparation and characterization

The synthesis of NiHCF active particles was performed by a co-precipitation method [8,41]. Briefly, a 200 mL solution of 24 mM $NiCl_2{\cdot}6H_2O$ (Alfa Aesar) and 12 mM $Na_4[Fe(CN)_6]{\cdot}10H_2O$ (Sigma Aldrich) each was drop-wise added to a (1% by volume) 1 M HCl solution. The reaction mixture was stirred at a 600 RPM for ≈12 h. Addition of HCl during the reaction has been reported to induce higher levels of crystallinity in the cubic lattice NiHCF structure [16]. The precipitate formed was washed three times with water in a vacuum filtration unit and the collected residue was dried overnight in a vacuum oven at 40 °C. The surface morphology of the NiHCF particles was studied using scanning electron microscopy (SEM). An elemental analysis was performed using energy-dispersive X-ray spectroscopy (EDS) to identify the elements in the active particles. The crystallinity of the NiHCF particles was assessed by powder X-ray diffraction (XRD) analysis, performed using a copper source for diffraction angles in the range of $10^o < 2\theta < 70^o$.

2.2. Electrode fabrication

The dried NiHCF powder was milled together with conductive carbon black (Cabot) and mixed with poly-tetrafluoroethylene (PTFE) (Sigma Aldrich) in ethanol as a solvent, in a weight ratio of 8:1:1 and subsequently cold-rolled into highly conductive, free-standing electrodes. The thickness of these electrodes was kept at 200 μm with an area of 20 cm^2. The electrodes were dried in an oven at 55 °C to evaporate any residual solvent left from the cold-rolling procedure. The weight of each electrode was between 0.42 and 0.45 g.

2.3. Electrochemical characterization and desalination

The galvanostatic intermittent titration was performed in a three-electrode cell configuration with NiHCF as the working electrode (WE), a platinum-coated titanium mesh as a counter electrode (CE) and a Ag/AgCl electrode as the reference electrode (RE) mounted close to the WE. The pH of the electrolyte solution (1 M solution of NaCl, $MgCl_2$, and $CaCl_2$) was kept at pH ≈ 3 by adding HCl. The equilibrium voltage was measured by interrupting the charging and discharging steps with an open circuit and measuring the cell voltage. In addition to assessing the capability of electrodes towards intercalation of cations, the three-electrode cell configuration was also utilized to control the charging degree, ϑ, of the electrodes. The assembly was used to set the ϑ values to either approximately 0 or 1 (by setting the WE potential to 1 or 0 V vs. Ag/AgCl, respectively).

The dependence of ionic selectivity of the electrodes on the relative concentration of mono- and divalent ions in the feed solution was explored by varying their concentration from equimolar mono- and divalent ions (optimum CDI concentration [42] of 20 mM) to an excess of divalent over monovalent ions (concentration ratio monovalent ions: divalent ions = 1: 3). These concentrations are given in Table 1. The desalination tests were run for solutions F1 – F6 with a symmetric CDI cell [17,40]. The solutions were fed to the two compartments from two separate 70 mL reservoirs. Before starting the tests, the CDI cell was

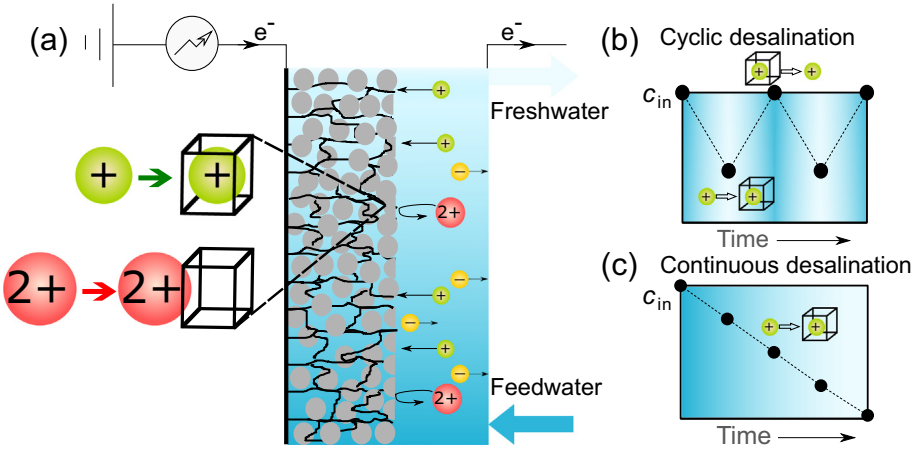

Fig. 1. Schematic overview of capacitive deionization with NiHCF electrodes in monovalent/divalent ion mixtures with two different operational modes. (a) Intercalation compartment from the two-compartment CDI cell [40] assembled with identical, free-standing NiHCF electrodes fed with feed water containing a mixture of Na^+, Ca^{2+}, Mg^{2+}. The redox-active NiHCF particles are present as grey agglomerates and the black lines running around them indicates the carbon black in the electrode. The schematic depicts the selective intercalation of monovalent cations in the cathode. The Cl^- electromigrates to the deintercalating compartment of the cell. (b) Schematic of the change in concentration of one feed reservoir paired with an electrode during the cyclic mode of desalination. The ion concentration decreases during the intercalation half-cycle and is restored during the deintercalation half-cycle. Therefore, the concentration remains unchanged after one full cycle. (c) Schematic presenting the change in concentration of the feed reservoir during the continuous mode of desalination. The ion concentration decreases with every half-cycle due to switching of the reservoir along with the electrode polarity. This leads to a permanent pairing of a reservoir with a cathode resulting in a continuous decrease in the concentration of ions.

Table 1
Composition of the feed F1 – F6 in the two-compartment deionization cell to investigate the dependence of electrode selectivity on the relative concentration of mono- and divalent ions in the electrolyte.

Feed number	Na^+ (mM)	Mg^{2+} (mM)	Ca^{2+} (mM)
F1	20	20	–
F2	20	–	20
F3	10	30	–
F4	10	–	30
F5	20	20	20
F6	40	40	40

short-circuited for 1 h to equilibrate the charge concentration in the electrodes with $\vartheta \approx 0$ and 1. As a result, ϑ in both the electrodes becomes ≈ 0.5. This step is necessary to ensure that the electrodes start operation from an identical state of charge, resulting in a symmetric deionization from both electrode compartments.

The (de)intercalation steps were performed under constant current, followed by a constant cell voltage applied via a potentiostat (n-stat, IVIUM technologies).

The desalination experiments were performed in two operational modes: *cyclic* and *continuous*. In cyclic desalination, the symmetrical cell was fed by two reservoirs containing identical solutions. A constant current of 10 A/m^2 (30 mA/g-NiHCF in both electrodes) was applied until the cell voltage reached a cut-off of 1.0 V. This was followed by applying a constant voltage of 1.0 V over the cell for 1 h. This concluded the first step. Once the electrodes were saturated, a current of -10 A/m^2 was applied in the opposite direction until the voltage reached a cut-off of -1 V. Following this, a voltage of -1 V was applied over the cell for 1 h to saturate the electrode. This second step completed one full cycle. One such cycle is given in Fig. S3 Supporting Information as a sample data set. The main characteristic of cyclic mode of operation is the periodic switching of electrode polarities only while keeping the feed reservoirs the same. In contrast, the continuous mode of operation allows for the switching of electrode polarities as well as the feed reservoirs. Therefore, after the first step of current and voltage application, the feed reservoirs are manually exchanged between the electrodes by simply changing the pipes connecting the cell compartments to the reservoirs. This manual swapping of reservoirs between the desalination steps is the defining feature of the continuous desalination. Once the electrodes reached equilibrium, samples were taken from both the reservoirs for ICP analysis. These equilibrium concentrations were used for selectivity calculations.

3. Results and discussion

The surface morphology of the NiHCF particles, observed under SEM (Fig. S1 Supporting Information), shows inter-particle agglomeration, and BET analysis shows a small surface area ($\approx$13 m^2/g). While such a small area would be highly detrimental for carbon-based electrodes in CDI, it does not hamper the performance of intercalation-based materials, in view of the different mode of ion storage, i.e. inside the lattice of the intercalation material rather than only near its surface. An elemental analysis of the NiHCF particles with ICP revealed the presence of Ni, Fe and Na in the ratio of 1.9:1.2:1. A deficiency in the amount of Na per formula unit, in comparison to the theoretical value (1:1:2) can be attributed to the fast precipitation of NiHCF during synthesis [16].

EDS mapping of powdered PBA revealed the presence of Ni, Fe and Na (in decreasing order) present in the crystal lattice which qualitatively supports the results obtained from the elemental analysis. The crystalline nature of the particles and the presence of cubic lattices were confirmed by the X-ray diffraction spectra, which display sharp peaks at positions consistent with those of materials in the *Fm3m* space groups (Fig. S1 Supporting Information), and consistent with literature [43].

To demonstrate the capability of the electrodes in intercalating mono- and divalent ions, a galvanostatic intermittent titration (GIT) [17,41,44,45] was performed with 1 M solutions of NaCl, $MgCl_2$ and $CaCl_2$ in a three-electrode cell configuration. The equilibrium voltages measured during the open-circuit regime of the titration is plotted against the charge input of the electrode in Fig. 2. The results indicate a single-phase (de)intercalation for both monovalent (Na^+) and divalent ion (Mg^{2+}) (data for Ca^{2+} in Fig. S2 Supporting Information) into the NiHCF particles of the electrodes, in line with literature [46,47]. A similar charge storage capacity of $\approx$55 mAh/g was measured for NiHCF electrodes in sodium electrolytes as in magnesium electrolytes, which is close to the reported maximum capacity of $\approx$60 mAh/g [17,47]. This result demonstrates the ability of the NiHCF electrodes to successfully (de)intercalate both mono- as well as divalent ions with similar, reversible capacities. The hysteresis observed in the voltage profiles for the larger Mg^{2+} is attributed to the rate-limiting dehydration step necessary for the intercalation of cations into the NiHCF lattice [48]. It has been reported that a dehydration step is necessary for the insertion of cations into the PB lattice [49–51]. Therefore, the larger Mg^{2+} requires more energy for dehydration to intercalate. This barrier to cation insertion into the NiHCF lattice results in the shifting of the intercalation curve to lower values of voltage, as measured in Mg electrolyte.

The electrode potentials measured during the GIT experiments in NaCl were correlated with the charge content of the electrode ϑ, a dimensionless number which ranges from 0 to 1 with 0 referring to the

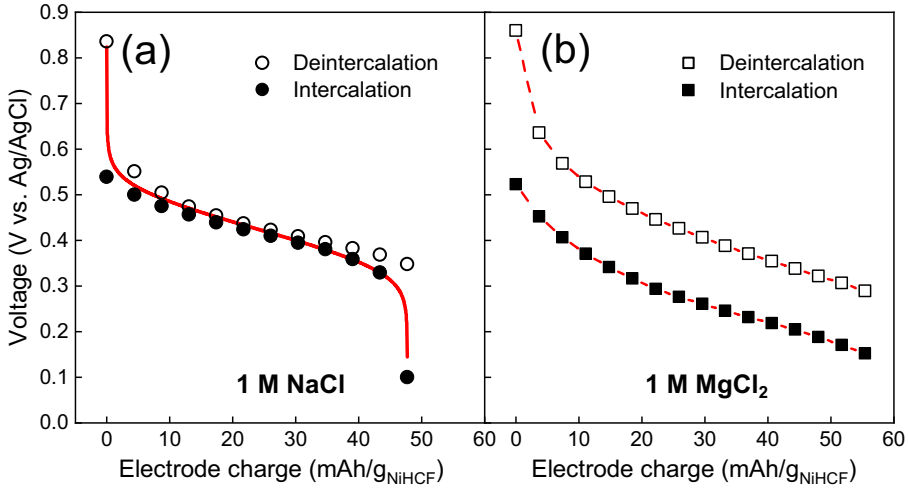

Fig. 2. Equilibrium voltage vs. electrode charge measured by GIT, for (a) 1 M NaCl, (b) $MgCl_2$ solution in a three-electrode cell with platinum coated titanium electrode as counter and a Ag/AgCl electrode as reference. Solid line in (a) represents the Frumkin adsorption isotherm fitted to the GIT data for monovalent Na^+ cation. Dashed line in (b) serves as a guide to the eye.

minimum cation content in the electrode (charged) and 1 referring to the maximum cation content in the electrode (discharged). The correlation follows from the Frumkin isotherm for monovalent cations [40],

$$E = E_{\text{ref}} - \frac{RT}{F}\left[\ln\frac{\vartheta}{1-\vartheta} - \ln\frac{c_+}{c_{\text{ref}}}\right] - g(\vartheta - 1/2), \quad (1)$$

where E_{ref} (reference potential dependent upon the intercalating ion and its interaction with the lattice of intercalation material), c_{ref}, and g (which is positive here and accounts for the inter-ionic repulsion in the intercalation particle) were 425 mV, 1 M, and 90 mV respectively, to get the best fit for both (de)intercalation voltage curves for NaCl, in line with previous reports [17]. The Frumkin adsorption isotherm however does not provide a similar insight into the (de)intercalation of divalent ions in the NiHCF lattice as in its current form, it does not account for the hysteresis associated with divalent ion insertion. Therefore, the isotherm can provide a qualitative insight into the (de)intercalation process of only the monovalent ions into the NiHCF electrodes.

The desalination tests with the symmetric CDI cell were performed in two operational modes referred to as *cyclic* and *continuous* desalination. The difference between these modes is reflected in the outlet concentration profiles obtained during these operations, presented in Fig. 1b & c. In the cyclic desalination mode, after the completion of the intercalation half-cycle, the electrodes were regenerated (deintercalated) in the same reservoir by reversing their polarities. Therefore, the concentration of ions in the reservoirs changed in a cyclic manner, as presented in Fig. 1b, because the reservoirs were permanently paired to one electrode regardless of its polarity. Therefore, after one full cycle, which comprised of an intercalation and a deintercalation step, the reservoir concentration was restored back to its original value.

The results of cyclic desalination on the feed solutions F1 – F5 in cyclic desalination are presented in Fig. 3. Feeds F1 – F4 contained a mixture of Na^+ and one of the divalent ions. Feed F5 contained all the three ions. The operation with a symmetric CDI cell resulted in a change in the concentration of Na^+, Ca^{2+}, and Mg^{2+} in the feed reservoirs. The closed circles, open triangles and squares represent the average change in concentration ($< \Delta c >$) of Na^+, Ca^{2+}, and Mg^{2+}, respectively, after every (de)intercalation half-cycle (See for the concentration profiles obtained in cyclic mode Figs. S4 & S5 in the Supporting Information). An average $\Delta[Na^+]$ of ≈ 7 mM was obtained after every half-cycle for every tested feed sample, regardless of its initial relative concentration with the divalent ions (Na^+/D^{2+} ratio, with D = Ca, Mg). This corresponds to 0.5 mmol-Na^+/(g-both electrodes) being removed in every half-cycle. In comparison, during the same desalination

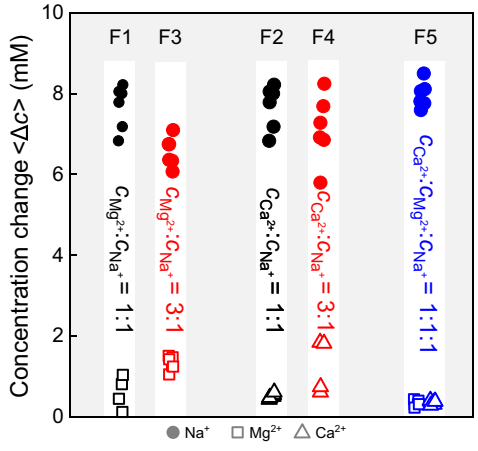

Fig. 3. Results of all the cyclic desalination experiments performed with the feed solutions F1 – F5. The average change in the concentration of Na^+ (closed circles), Mg^{2+} (open squares), and Ca^{2+} (open triangles) is plotted on the y-axis. The separation factor β, calculated by Eq. (2), was found to be 15 ± 2 for binary ion mixtures (F1 – F4) and ≈ 25 for ionic mixture of all three ions (F5).

tests, the uptake of the divalent ions by the electrodes remained consistently low at ≈0.1 mmol/(g-both electrodes) i.e. $\Delta[Ca^{2+}]$ and $\Delta[Mg^{2+}]$ were in the 0.5–1 mM range. The data presented in Fig. 3 demonstrate the high affinity of the NiHCF particles towards monovalent ions, which is quantified with a separation factor [25,28,34], β, calculated as

$$\beta_{M/D} = \left(\frac{c_{M,\text{initial}} - c_{M,\text{final}}}{c_{D,\text{initial}} - c_{D,\text{final}}}\right)\left(\frac{c_{D,\text{initial}}}{c_{M,\text{initial}}}\right), \quad (2)$$

where M and D represent the monovalent (Na^+) and divalent (Mg^{2+} or Ca^{2+}) ions, $c_{M,\text{ initial}}$, $c_{M,\text{ final}}$, $c_{D,\text{ initial}}$, and $c_{D,\text{ final}}$ are the concentrations of the mono- and divalent ions in the beginning and at the end of the intercalation half-cycle, respectively. A high average $\beta \approx 15$ was measured for feeds with equimolar ion concentration (F1, F3) and feeds with the concentration of divalent ions three times as much as that of the monovalent ions (F2, F4). Such a β value clearly indicates a strong preference of NiHCF electrodes towards monovalent Na^+. This trend is in contrast to values reported for carbon electrodes which are more selective towards divalent ions: β values of ≈7 and 24 were reported towards Ca^{2+} over Na^+ from a 1:5 Ca^{2+}:Na^+ solution for different adsorption times [52]; a β value of ≈1.5 was reported towards Ca^{2+} over Na^+ from a 1:1 Ca^{2+}:Na^+ solution [53]. Furthermore, the obtained selectivity here for Na^+ over Mg^{2+} and Ca^{2+}, $13 < \beta < 17$, is twice as high in comparison to a CDI cell, $6 < \beta < 8$, constructed with $Na_{0.44\text{-}x}MnO_2$, another widely used intercalation material [26]. This selectivity is also comparable to other systems such as electrodialysis in which ion-selective membranes are used to achieve preferential ion adsorption [54,55].

In addition to the selective removal of Na^+ from a binary mixture with Mg^{2+} and Ca^{2+}, the ability of the NiHCF electrodes to selectively remove Na^+ from an equimolar mixture of all three ions was also investigated. The feed F5 was desalinated to test the influence of the presence of multiple ions on the selectivity of the NiHCF electrodes. In this case, an average β value ≈ 20 and 25 was obtained for Na^+ over Ca^{2+} and Mg^{2+} respectively. Similar results in CDI have been reported for preferential removal of Cs^+ over Mg^{2+} with titanium disulfide as intercalation materials [56]. However, it must be pointed out that the monovalent ion removed in this study is Na^+, the second largest hydrated alkali metal ion and considerably larger than Cs^+. In addition, these β values also indicate that the presence of more than one divalent ion in the feed has no adverse influence on the Na-removal performance of the electrodes. To the contrary, the selective ion separation becomes more pronounced with all three ions present in the solution. An increase in the number and type of divalent ions that are difficult to intercalate may work in the favor of Na^+ resulting in its preferential removal from a ternary mixture. A similar phenomenon of competition between intercalating and non-intercalating ions has been reported before [57]. However, we do not have experimental evidence to support this claim and therefore, this only remains a hypothesis.

It can be concluded that within the bounds of the tested concentrations of the three ions in the feed solution, the NiHCF active particles remain highly selective towards Na^+ ions. Tables S1–S6 in the Supporting Information provide all the information of the achieved concentration reduction, $< \Delta c >$, calculated for each ion for every intercalation half-cycle performed with the feeds F1 – F5 for the left and the right compartments of the symmetric CDI cell. Charge efficiency during intercalation Λ, calculated as the ratio of ion uptake and charge input, was found to be between 85 and 95%. These values have been tabulated and provided in Table S7 of the Supporting Information.

The second mode of operation, namely continuous desalination, is of more practical relevance because it results in uninterrupted desalination of the feed reservoirs. This mode requires a manual switching of the reservoirs between the cell compartments, simultaneously with the switch in the electrode polarities. As a result, reservoirs are permanently paired with either a positive or a negative electrode, resulting in

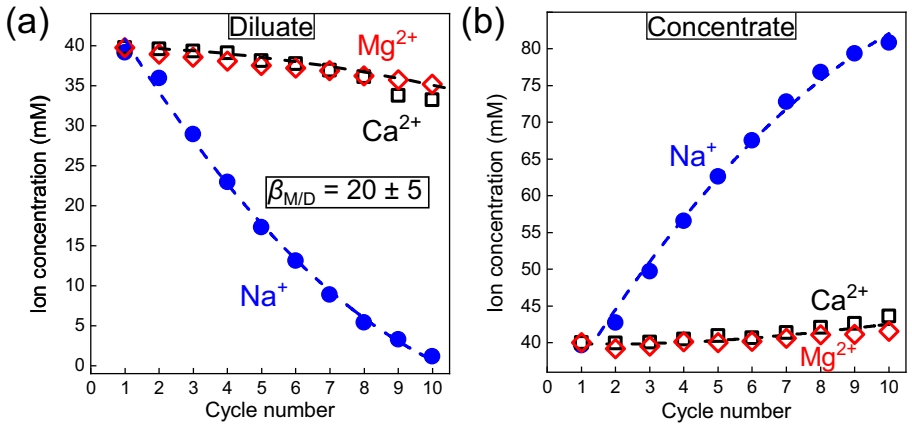

Fig. 4. Continuous desalination via symmetric CDI cell with identical NiHCF electrodes (a) Result from the intercalation compartment (diluate) during the continuous desalination of F6, containing 40 mM each of Na^+, Mg^{2+}, and Ca^{2+}. (b) Result from the deintercalation compartment (concentrate) during the continuous desalination of F6. Average separation factor of 20 ± 5 between monovalent (Na^+) and divalent (Ca^{2+} and Mg^{2+}) ions was obtained during continuous desalination of F6. The dashed lines serve as a guide to the eye.

a continuous deionization or enrichment of the reservoir. The symmetric nature of the CDI cell becomes highly desirable because desalination can continue without being interrupted for electrode regeneration. A schematic of the expected concentration profile in the depleted reservoir (diluate) is shown in Fig. 1c. In contrast to cyclic desalination, this mode of operation permanently removes ions from one reservoir and concentrates them in the other reservoir (Fig. S6 Supporting Information).

Average concentrations (from two separate runs) of Na^+, Ca^{2+}, and Mg^{2+} in the diluate and the concentrate output streams from the cell, during the desalination experiments performed in continuous mode, are reported in Fig. 4. The decrease and increase in the concentration of the ions obtained in either of the reservoirs supports the claim of symmetric operation of the presented CDI cell configuration. It can be seen from Fig. 4a that > 85% of Na^+ (a reduction in concentration from 40 mM to 5 mM) was removed from the solution within the first 7 half-cycles. During these 7 half-cycles, < 10% of Ca^{2+} and Mg^{2+} was removed. On an average, a separation factor of 20 ± 5 was obtained for Na^+ over Ca^{2+} and Mg^{2+}. Remarkably, there was no drastic reduction in the preference towards Na^+ even after its concentration in the mixture was reduced by > 90%, as evident from Fig. 4a. Therefore, it can be inferred that the selectivity of NiHCF electrodes towards Na^+ does not strongly depend on the concentration of Na^+ in the ionic mixture.

Fig. 4b presents the concentration of all the ions in the concentrate reservoir. The decrease in the diluate concentration is associated with an equivalent increase in the number of ions in the concentrate. This clearly support the claim of symmetric CDI operation with identical NiHCF electrodes. As a finer point it may, additionally, be noted that a slight difference in the performance of the two electrodes may arise from an unequal distribution of the cell voltage between them, or an asymmetric charging degree, ϑ, in the electrodes, leading to an incomplete use of one half of the desalination cell.

Another consequence of the (de)intercalation of cations is dissolution of the metallic components of the lattice in the treated water. This results in the loss of capacity of the electrodes over time. Such losses have previously been reported in literature as well [42,53]. It has been recently reported that Mg^{2+} can replace Ni^{2+} in the lattice resulting in dissolution of the iron centres of the lattice as well [51]. This can enhance the fade in capacity of the electrodes. Fig. S7 gives the concentration profile of nickel and iron in the treated water for both cyclic as well as continuous desalination modes. While the continuous mode results in the accumulation of nickel and iron in the concentrate and the diluate chamber, respectively. In contrast, the build-up of nickel during the cyclic desalination mode is slowed down by its partial adsorption by the electrode. This further shows the ability of the NiHCF electrodes to intercalate ions of multiple valences.

The preference of NiHCF electrodes towards monovalent ions was also tested after the electrodes were run for 200 cycles. The concentration profile obtained from this experiment is given in the Fig. S8 of the Supplementary Information. The preference towards monovalent Na^+ ions was clearly preserved. However, after 200 cycles, the divalent ions were removed in larger amounts (≈20%) in comparison to the time when fresh electrodes were used (≈10%). In the same interval, Na^+ concentration dropped by ≈90%. This resulted in a small reduction in the separation factor β for monovalent Na^+ over divalent Ca^{2+} and Mg^{2+} to ≈11 ± 4 in comparison to the value of 20 ± 5 obtained using fresh electrodes, as mentioned in Fig. 4. Therefore, it can be concluded that as far as long-term selectivity is considered, the preference of NiHCF electrodes towards monovalent ions over divalent ions was preserved.

The selectivity of NiHCF electrodes towards Na^+ from a mixture containing Ca^{2+} and Mg^{2+} ions can be primarily attributed to their different dehydration energies with divalent ions having higher energies than monovalent ions [58] which follows from their hydrated ionic radii: Na^+ = 3.58 Å; Ca^{2+} = 4.12 Å; Mg^{2+} = 4.28 Å [59]. The intercalation of these ions in the NiHCF lattice requires partial dehydration of the inserting ion [49]. Thus, a larger dehydration energy would make the intercalation of a divalent ion thermodynamically unfavorable in comparison to the monovalent ion, present in the ionic mixture. Another, entropic, barrier to the intercalation of divalent ions in the NiHCF lattice is their requirement for the simultaneous reduction of two Fe^{3+} atoms in the lattice. In contrast, Na^+ intercalation only requires one Fe^{3+} center to be reduced. These combined effects yield the high selectivity of the NiHCF electrodes observed here for monovalent Na^+ ion.

4. Conclusion

A symmetrical CDI cell was assembled with identical electrodes fabricated with NiHCF as active particles. Six different concentrations of Na^+, Ca^{2+}, and Mg^{2+} were desalinated in cyclic and continuous mode. In the cyclic mode, high values of the selectivity factor (calculated as the ratio of the amount of monovalent and divalent ions removed relative to their initial concentration) $\beta_{Na/Ca}$ and $\beta_{Na/Mg}$, between 13 and 17 were obtained for the feed solution containing a mixture of Na^+ with Ca^{2+} and Mg^{2+}, respectively in the ratio of 1:1 (equimolar) and 1:3 (divalent ions three times as much as the monovalent ions). The selective removal of Na^+ remained unaffected by the increase in the concentration of divalent ions in the solution. An equimolar mixture of all three ions, when desalinated in cyclic mode, resulted in a high average $\beta \approx 20$ and 25 towards Na^+ over the divalent Ca^{2+} and Mg^{2+} ions, respectively. During the continuous desalination of the equimolar solution containing all three ions, a symmetrical increase and decrease in ion concentration was obtained in the reservoirs feeding the two compartment CDI cell. In addition, > 95% of all Na^+ ions was removed from the solution while only 10% of Mg^{2+} ions

and Ca^{2+} ions was removed. The average β varied between 15 and 25 for Na^+ over Ca^{2+} and Mg^{2+}. Furthermore, the preference towards Na^+ did not decrease with its decreasing concentration in the diluate stream out of the continuous desalination cell. Therefore, the developed electrochemical system serves as an elegant solution for continuous, highly selective removal of monovalent ions from a mixture of monovalent and divalent ions via capacitive deionization.

CRediT authorship contribution statement

Kaustub Singh: Conceptualization, Investigation, Formal analysis, Data curation, Writing - original draft. **Zexin Qian:** Conceptualization, Investigation, Formal analysis, Data curation, Writing - review & editing. **P.M. Biesheuvel:** Data curation, Writing - review & editing. **Han Zuilhof:** Data curation, Writing - review & editing. **Slawomir Porada:** Formal analysis, Writing - review & editing. **Louis C.P.M. de Smet:** Supervision, Data curation, Writing - review & editing.

Acknowledgment

This work was supported by the European Union Horizon 2020 research and innovation program (ERC Consolidator Grant to L.d.S., Agreement No. 682444) and was performed in collaboration with Wetsus, European Centre of Excellence for Sustainable Water Technology. Wetsus is co-funded by the Dutch Ministry of Economic Affairs and Climate Policy, the Northern Netherlands Provinces, and the Province of Fryslan. The authors thank the participants of the research theme Capacitive Deionization for fruitful discussions and financial support, Mr. Barend van Lagen (WUR) for XRD experiments, and Dr. Prashanth Kumar (Wetsus) for SEM and EDS measurements.

Declaration of competing interest

All authors are aware of the submission and agree to its publication. The authors declare no conflict of interest.

Appendix A. Supplementary data

Supplementary data to this article can be found online at https://doi.org/10.1016/j.desal.2020.114346.

References

[1] K. Singh, S. Porada, H.D. de Gier, P.M. Biesheuvel, L.C.P.M. de Smet, Timeline on the application of intercalation materials in capacitive deionization, Desalination 455 (2019) 115–134, https://doi.org/10.1016/J.DESAL.2018.12.015.
[2] S. Porada, R. Zhao, A. Van Der Wal, V. Presser, P.M. Biesheuvel, Review on the science and Technology of Water Desalination by capacitive deionization, Prog. Mater. Sci. 58 (8) (2013) 1388–1442, https://doi.org/10.1016/j.pmatsci.2013.03.005.
[3] Z.-H. Huang, Z. Yang, F. Kang, M. Inagaki, Carbon electrodes for capacitive deionization, J. Mater. Chem. A 5 (2) (2017) 470–496, https://doi.org/10.1039/C6TA06733F.
[4] M.E. Suss, S. Porada, X. Sun, P.M. Biesheuvel, J. Yoon, V. Presser, Water desalination via capacitive deionization: what is it and what can we expect from it? Energy Environ. Sci. 8 (8) (2015) 2296–2319, https://doi.org/10.1039/C5EE00519A.
[5] Y. Liu, C. Nie, X. Liu, X. Xu, Z. Sun, L. Pan, Review on carbon-based composite materials for capacitive deionization, RSC Adv. 5 (20) (2015) 15205–15225, https://doi.org/10.1039/c4ra14447c.
[6] S. Porada, L. Borchardt, M. Oschatz, M. Bryjak, J.S. Atchison, K.J. Keesman, S. Kaskel, P.M. Biesheuvel, V. Presser, Direct prediction of the desalination performance of porous carbon electrodes for capacitive deionization, Energy Environ. Sci. 6 (12) (2013) 3700–3712, https://doi.org/10.1039/c3ee42209g.
[7] C. Kim, P. Srimuk, J. Lee, S. Fleischmann, M. Aslan, V. Presser, Influence of pore structure and cell voltage of activated carbon cloth as a versatile electrode material for capacitive deionization, Carbon N. Y. 122 (2017) 329–335, https://doi.org/10.1016/j.carbon.2017.06.077.
[8] Y. Lu, L. Wang, J. Cheng, J.B. Goodenough, Prussian blue: a new framework of electrode materials for sodium batteries, Chem. Commun. 48 (52) (2012) 6544–6546, https://doi.org/10.1039/c2cc31777j.
[9] A. Paolella, C. Faure, V. Timoshevskii, S. Marras, G. Bertoni, A. Guerfi, A. Vijh, M. Armand, K. Zaghib, A review on Hexacyanoferrate-based materials for energy storage and smart windows: challenges and perspectives, J. Mater. Chem. A 5 (2017) 18919–18932, https://doi.org/10.1039/c7ta05121b.
[10] F. Ma, Q. Li, T. Wang, H. Zhang, G. Wu, Energy storage materials derived from Prussian blue analogues, Sci. Bull. 62 (5) (2017) 358–368, https://doi.org/10.1016/j.scib.2017.01.030.
[11] J. Lee, S. Kim, J. Yoon, Rocking chair desalination battery based on Prussian blue electrodes, ACS Omega 2 (4) (2017) 1653–1659, https://doi.org/10.1021/acsomega.6b00526.
[12] S. Kim, J. Lee, C. Kim, J. Yoon, $Na_2FeP_2O_7$ as a novel material for hybrid capacitive deionization, Electrochim. Acta 203 (2016) 265–271, https://doi.org/10.1016/j.electacta.2016.04.056.
[13] M. Pasta, C.D. Wessells, Y. Cui, F. La Mantia, A desalination battery, Nano Lett. 12 (2) (2012) 839–843, https://doi.org/10.1021/nl203889e.
[14] M.E. Suss, V. Presser, Water desalination with energy storage electrode materials, Joule 2 (1) (2018) 25–35, https://doi.org/10.1016/j.joule.2017.12.010.
[15] B.W. Byles, B. Hayes-Oberst, E. Pomerantseva, Ion removal performance, structural/compositional dynamics, and electrochemical stability of layered manganese oxide electrodes in hybrid capacitive deionization, ACS Appl. Mater. Interfaces 10 (38) (2018) 32313–32322.
[16] J.H. Lee, G. Ali, D.H. Kim, K.Y. Chung, Metal-organic framework cathodes based on a vanadium Hexacyanoferrate Prussian blue analogue for high-performance aqueous rechargeable batteries, Adv. Energy Mater. 7 (2) (2017), https://doi.org/10.1002/aenm.201601491.
[17] S. Porada, A. Shrivastava, P. Bukowska, P.M. Biesheuvel, K.C. Smith, Nickel Hexacyanoferrate electrodes for continuous Cation intercalation desalination of brackish water, Electrochim. Acta 255 (2017) 369–378, https://doi.org/10.1016/j.electacta.2017.09.137.
[18] L. Guo, R. Mo, W. Shi, Y. Huang, Z.Y. Leong, M. Ding, F. Chen, H.Y. Yang, A Prussian blue anode for high performance electrochemical deionization promoted by the faradaic mechanism, Nanoscale 9 (35) (2017) 13305–13312, https://doi.org/10.1039/c7nr03579a.
[19] Y. Liu, Y. Qiao, W. Zhang, Z. Li, X. Ji, L. Miao, L. Yuan, X. Hu, Y. Huang, Sodium Storage in Na-Rich $Na_xFeFe(CN)_6$ nanocubes, Nano Energy 12 (2015) 386–393, https://doi.org/10.1016/j.nanoen.2015.01.012.
[20] A.A. Karyakin, Prussian Blue and its Analogues: Electrochemistry and Analytical Applications, 13 (2001), pp. 813–819.
[21] M.E. Suss, Size-based ion selectivity of micropore electric double layers in capacitive deionization electrodes, J. Electrochem. Soc. 164 (9) (2017) E270–E275, https://doi.org/10.1149/2.1201709jes.
[22] H. Yoon, J. Lee, S.R. Kim, J. Kang, S. Kim, C. Kim, J. Yoon, Capacitive deionization with Ca-alginate coated-carbon electrode for hardness control, Desalination 392 (2016) 46–53, https://doi.org/10.1016/j.desal.2016.03.019.
[23] P. Nativ, O. Lahav, Y. Gendel, Separation of divalent and monovalent ions using flow-electrode capacitive deionization with Nanofiltration membranes, Desalination 425 (2018) 123–129, https://doi.org/10.1016/j.desal.2017.10.026.
[24] L. Wang, S. Lin, Mechanism of selective ion removal in membrane capacitive deionization for water softening, Environ. Sci. Technol. 53 (10) (2019) 5797–5804, https://doi.org/10.1021/acs.est.9b00655.
[25] T. Kim, C.A. Gorski, B.E. Logan, Ammonium removal from domestic wastewater using selective battery electrodes, Environ. Sci. Technol. Lett. 5 (9) (2018) 578–583, https://doi.org/10.1021/acs.estlett.8b00334.
[26] S. Kim, H. Yoon, D. Shin, J. Lee, J. Yoon, Electrochemical selective ion separation in capacitive deionization with sodium manganese oxide, J. Colloid Interface Sci. 506 (2017) 644–648, https://doi.org/10.1016/j.jcis.2017.07.054.
[27] W. Chen, X.H. Xia, Highly stable nickel Hexacyanoferrate nanotubes for electrically switched ion exchange, Adv. Funct. Mater. 17 (15) (2007) 2943–2948, https://doi.org/10.1002/adfm.200700015.
[28] D.I. Oyarzun, A. Hemmatifar, J.W. Palko, M. Stadermann, J.G. Santiago, Ion selectivity in capacitive deionization with functionalized electrode: theory and experimental validation, Water Res. X 1 (2018) 100008, , https://doi.org/10.1016/j.wroa.2018.100008.
[29] S.J. Seo, H. Jeon, J.K. Lee, G.Y. Kim, D. Park, H. Nojima, J. Lee, S.H. Moon, Investigation on removal of hardness ions by capacitive deionization (CDI) for water softening applications, Water Res. 44 (7) (2010) 2267–2275, https://doi.org/10.1016/j.watres.2009.10.020.
[30] D.H. Lee, T. Ryu, J. Shin, J.C. Ryu, K.S. Chung, Y.H. Kim, Selective Lithium recovery from aqueous solution using a modified membrane capacitive deionization system, Hydrometallurgy 173 (2017) 283–288, https://doi.org/10.1016/j.hydromet.2017.09.005.
[31] C.J. Gabelich, T.D. Tran, I.H. Suffet, Electrosorption of inorganic salts from aqueous solution using carbon aerogels, Environ. Sci. Technol. 36 (13) (2002) 3010–3019, https://doi.org/10.1021/es0112745.
[32] T. Ikeshoji, Separation of alkali metal ions by intercalation into a Prussian blue electrode, J. Electrochem. Soc. 133 (10) (1986) 2108–2109, https://doi.org/10.1149/1.2108350.
[33] A.B. Bocarsly, S. Sinha, Effects of surface structure on electrode charge transfer properties. Induction of ion selectivity at the chemically Derivatized Interface, J. Electroanal. Chem. 140 (1) (1982) 167–172, https://doi.org/10.1016/0368-1874(82)85310-0.
[34] S.D. Rassat, J.H. Sukamto, R.J. Orth, M.A. Lilga, R.T. Hallen, Development of an electrically switched ion exchange process for selective ion separations, Sep. Purif. Technol. 15 (3) (1999) 207–222, https://doi.org/10.1016/S1383-5866(98)00102-6.
[35] M.A. Lilga, R.J. Orth, J.P.H. Sukamto, S.M. Haight, D.T. Schwartz, Metal ion separations using electrically switched ion exchange, Sep. Purif. Technol. 11 (3)

(1997) 147–158, https://doi.org/10.1016/S1383-5866(97)00017-8.
[36] D.L. Suarez, J.D. Wood, S.M. Lesch, Effect of SAR on water infiltration under a sequential rain-irrigation management system, Agric. Water Manag. 86 (1–2) (2006) 150–164, https://doi.org/10.1016/j.agwat.2006.07.010.
[37] J.L. Zhang, T.J. Flowers, S.M. Wang, Mechanisms of sodium uptake by roots of higher plants, Plant Soil 326 (1–2) (2010) 45, https://doi.org/10.1007/s11104-009-0076-0.
[38] A. Läuchli, S.R. Grattan, Plant growth and development under salinity stress, Advances in Molecular Breeding toward Drought and Salt Tolerant Crops, 2007, pp. 1–32, , https://doi.org/10.1007/978-1-4020-5578-2_1.
[39] K.C. Smith, R. Dmello, Na-ion desalination (NID) enabled by Na-blocking membranes and symmetric Na-intercalation: porous-electrode modeling, J. Electrochem. Soc. 163 (3) (2016) A530–A539, https://doi.org/10.1149/2.0761603jes.
[40] K. Singh, H.J.M. Bouwmeester, L. de Smet, M.Z. Bazant, P.M. Biesheuvel, Theory of water desalination with intercalation materials, Phys. Rev. Appl. 9 (6) (2018) 64036–64045.
[41] C.D. Wessells, M.T. McDowell, S.V. Peddada, M. Pasta, R.A. Huggins, Y. Cui, Tunable reaction potentials in open framework nanoparticle battery electrodes for grid-scale energy storage, ACS Nano 6 (2) (2012) 1688–1694, https://doi.org/10.1021/nn204666v.
[42] S.A. Hawks, A. Ramachandran, S. Porada, P.G. Campbell, M.E. Suss, P.M. Biesheuvel, J.G. Santiago, M. Stadermann, Performance metrics for the objective assessment of capacitive deionization systems, Water Res. 152 (2018) 126–137, https://doi.org/10.1016/j.watres.2018.10.074.
[43] Y. Mizuno, M. Okubo, E. Hosono, T. Kudo, H. Zhou, K. Oh-Ishi, Suppressed activation energy for interfacial charge transfer of a Prussian blue analog thin film electrode with hydrated ions (Li^+, Na^+, and Mg^{2+}), J. Phys. Chem. C 117 (21) (2013) 10877–10882, https://doi.org/10.1021/jp311616s.
[44] M. Asai, A. Takahashi, K. Tajima, H. Tanaka, M. Ishizaki, M. Kurihara, T. Kawamoto, Effects of the variation of metal substitution and electrolyte on the electrochemical reaction of metal Hexacyanoferrates, RSC Adv. 8 (65) (2018) 37356–37364, https://doi.org/10.1039/c8ra08091g.
[45] C.D. Wessells, S.V. Peddada, M.T. McDowell, R.A. Huggins, Y. Cui, The effect of insertion species on nanostructured open framework Hexacyanoferrate battery electrodes, J. Electrochem. Soc. 159 (2) (2012) A98–A103, https://doi.org/10.1149/2.060202jes.
[46] R.Y. Wang, C.D. Wessells, R.A. Huggins, Y. Cui, Highly reversible open framework Nanoscale electrodes for divalent ion batteries, Nano Lett. 13 (11) (2013) 5748–5752, https://doi.org/10.1021/nl403669a.
[47] C.D. Wessells, S.V. Peddada, R.A. Huggins, Y. Cui, Nickel Hexacyanoferrate nanoparticle electrodes for aqueous sodium and potassium ion batteries, Nano Lett. 11 (12) (2011) 5421–5425, https://doi.org/10.1021/nl203193q.
[48] F. Scholz, A. Dostal, The formal potentials of solid metal hexacyanometalates, Angew. Chemie Int. Ed. 34 (2324) (2004) 2685–2687, https://doi.org/10.1002/anie.199526851.
[49] R.Y. Wang, B. Shyam, K.H. Stone, J.N. Weker, M. Pasta, H.W. Lee, M.F. Toney, Y. Cui, Reversible multivalent (monovalent, divalent, trivalent) ion insertion in open framework materials, Adv. Energy Mater. 5 (12) (2015) 1–10, https://doi.org/10.1002/aenm.201401869.
[50] J.J. García-Jareño, D. Giménez-Romero, F. Vicente, C. Gabrielli, M. Keddam, H. Perrot, EIS and ac-Electrogravimetry study of PB films in KCl, NaCl, and CsCl aqueous solutions, J. Phys. Chem. B 107 (41) (2003) 11321.
[51] A. Shrivastava, S. Liu, K.C. Smith, Linking capacity loss and retention of nickel Hexacyanoferrate to a two-site intercalation mechanism for aqueous Mg^{2+} and Ca^{2+} ions, Phys. Chem. Chem. Phys. 21 (2019) 20177, , https://doi.org/10.1039/c9cp04115j.
[52] R. Zhao, M. Van Soestbergen, H.H.M. Rijnaarts, A. Van der Wal, M.Z. Bazant, P.M. Biesheuvel, Time-dependent ion selectivity in capacitive charging of porous electrodes, J. Colloid Interface Sci. 384 (1) (2012) 38–44.
[53] C.-H. Hou, C.-Y. Huang, A comparative study of Electrosorption selectivity of ions by activated carbon electrodes in capacitive deionization, Desalination 314 (2013) 124–129.
[54] F. Radmanesh, T. Rijnaarts, A. Moheb, M. Sadeghi, W.M. de Vos, Enhanced selectivity and performance of heterogeneous Cation exchange membranes through addition of Sulfonated and protonated Montmorillonite, J. Colloid Interface Sci. 533 (2019) 658–670, https://doi.org/10.1016/j.jcis.2018.08.100.
[55] T. Rijnaarts, D.M. Reurink, F. Radmanesh, W.M. de Vos, K. Nijmeijer, Layer-by-layer coatings on ion exchange membranes: effect of multilayer charge and hydration on monovalent ion Selectivities, J. Memb. Sci. 570 (2019) 513–521, https://doi.org/10.1016/j.memsci.2018.10.074.
[56] P. Srimuk, J. Lee, S. Fleischmann, M. Aslan, C. Kim, V. Presser, Potential-dependent, switchable ion selectivity in aqueous media using titanium disulfide, ChemSusChem 11 (13) (2018) 2091–2100, https://doi.org/10.1002/cssc.201800452.
[57] S. Shanbhag, Y. Bootwala, J.F. Whitacre, M.S. Mauter, Ion transport and competition effects on $NaTi_2(PO_4)_3$ and $Na_4Mn_9O_{18}$ selective insertion electrode performance, Langmuir 33 (44) (2017) 12580–12591, https://doi.org/10.1021/acs.langmuir.7b02861.
[58] M. Peschke, A.T. Blades, P. Kebarle, Hydration energies and entropies for Mg^{2+}, Ca^{2+}, Sr^{2+}, and Ba^{2+} from gas-phase ion − water molecule equilibria determinations, J. Phys. Chem. A 102 (48) (2002) 9978–9985, https://doi.org/10.1021/jp9821127.
[59] E.R. Nightingale, Phenomenological theory of ion solvation. Effective radii of hydrated ions, J. Phys. Chem. 63 (9) (1959) 1381–1387.